

Isochronal superposition and density scaling of the α -relaxation from pico- to millisecond

Henriette Wase Hansen,^{1,2} Bernhard Frick,² Simone Capaccioli,³ Alejandro Sanz,¹ and Kristine Niss^{1,a)}

¹*Glass and Time, IMFUFA, Department of Science and Environment, Roskilde University, P.O. Box 260, DK-4000 Roskilde, Denmark*

²*Institut Laue-Langevin, 71 Avenue des Martyrs, CS 20156, 38042 Grenoble Cedex 9, France*

³*Dipartimento di Fisica, Università di Pisa, Largo B. Pontecorvo 3, I-56127 Pisa, Italy*

(Received 9 September 2018; accepted 31 October 2018; published online 6 December 2018)

The relaxation dynamics in two van der Waals bonded liquids and one hydrogen-bonding molecular liquid are studied as a function of pressure and temperature by incoherent neutron scattering using simultaneous dielectric spectroscopy. The dynamics are studied in a range of alpha relaxation times from pico- to milliseconds, primarily in the equilibrium liquid state. In this range, we find that isochronal superposition and density scaling work not only for the two van der Waals liquids but also for the hydrogen-bonding liquid, though the density scaling exponent is much smaller for the latter. Density scaling and isochronal superposition are seen to break down for intra-molecular dynamics when it is separated in time from the alpha relaxation, in close agreement with previous observations from molecular dynamics simulations. *Published by AIP Publishing.* <https://doi.org/10.1063/1.5055665>

I. INTRODUCTION

A full understanding of the dynamics in liquids is still a pending challenge in chemical physics research.^{1,2} A better understanding of the dynamics has implications not only for small organic molecular liquids as will be presented in this paper but also for other materials such as polymers, proteins, and metals.^{3–5} The dynamics in liquids span many orders of time scales from the equilibrium liquid above the melting temperature, where relaxation times are shorter than nanoseconds, to the viscous slowing down in the supercooled state as the glass transition is approached and the α -relaxation reaches 100 s.

Slowing down of the liquid dynamics and the glass transition are traditionally observed by cooling a liquid, but they are also seen upon compression. New insight into liquid dynamics has been gained in the past decades by introducing pressure as an additional variable to temperature.⁶

Tölle⁷ observed isochronal superposition of neutron spectra on picosecond time scales. Isochronal superposition is the observation of an invariance of the spectral shape and linewidth along lines of constant relaxation time in the temperature-pressure phase diagram.⁸ The observation of isochronal superposition implies that the spectral shape is determined by the relaxation time or that it is controlled by the same underlying mechanism.⁹

Density scaling is another experimental observation from pressure experiments based on the ideas from the soft repulsive potential.^{7,10} It was shown for several systems that the viscosity or the relaxation time as a function of temperature and pressure could be brought to collapse when expressed in

terms of the parameter $\Gamma = \rho^\gamma/T$ (Refs. 6, 11, and 12), where γ is a material specific constant. Density scaling has since been shown to apply to numerous different systems and implies that in these systems the relaxation time is governed by the parameter Γ .

A complete understanding of the dynamics in liquids must encompass pressure behavior and therefore also the observations of density scaling and isochronal superposition from pressure experiments. One proposed approach is to assume the existence of isomorphs as suggested by isomorph theory.^{13,14} The basic idea is that two thermodynamic state points as a function of atomic coordinates and density are isomorphic if they have the same potential energy landscape upon scaling of the atomic coordinates.¹³ This gives rise to curves in the phase diagram along which dynamics on all time scales presented in reduced dimensionless units are invariant. The dynamics in this view are on all time scales determined by the same control parameter, Γ , which in the simplest case is given by $\Gamma = \rho^\gamma/T$. Density scaling and isochronal superposition are therefore natural consequences of isomorphs. A conjecture of isomorph theory is that it only works for R -simple systems, i.e., systems that in molecular dynamics simulations show a strong correlation between the potential energy and the virial.^{15–18} From an experimental point of view, the conjecture is that the idea of R -simple systems is manifested in systems without directional bonding or competing interactions. Moreover, isomorph theory only describes inter-molecular interactions, and to be certain to exclude intra-molecular modes, we consider experimental candidates for simple liquids to be those with no large secondary relaxations.

From dielectric spectroscopy, it has previously been shown that isochronal superposition works better for van der Waals liquids than for hydrogen-bonding liquids,¹⁹ although several other studies also with dielectrics^{20–23} and molecular

^{a)}Electronic mail: kniss@ruc.dk

dynamics simulations²⁴ have shown that density scaling and isochronal superposition apply to hydrogen-bonding systems as well.

In a recent paper, we showed that the picosecond dynamics along the glass transition as a function of temperature and pressure, i.e., fast relaxations and vibrations that are completely separated from the α -relaxation, measured with neutron spectroscopy were invariant for two simple van der Waals liquids.²⁵ For these simple liquids, we observed isochronal superposition of the dynamics separated by 14 orders of magnitude, which was interpreted as a genuine signature of these liquids having isomorphs. The implication of this finding is that for simple liquids with isomorphs, the phase diagram can be reduced to just one dimension with the control parameter Γ , in contrast to an experimentalist's normal temperature-pressure phase diagram. A hydrogen-bonding liquid with directional bonding was chosen to test a more complex system in contrast to the simple van der Waals liquids. We showed how the relation between picosecond dynamics and the glass transition broke down for the hydrogen-bonding complex liquid, in agreement with the predictions from isomorph theory.

Most previous experimental studies of glass-forming liquids, also the ones at short time scales as probed, for example, by neutron spectroscopy, take place in the viscous or supercooled liquid, thus, in the proximity of the glass transition. In this paper, we focus on the dynamics in the liquid state with fast α -relaxation times. We expand the test of density scaling and isochronal superposition to experimental time scales in the equilibrium liquid when the α -relaxation is on the same time scale as neutron spectroscopy. These fast sub-nanosecond time scales are also accessible with molecular dynamics computer simulations.

We apply for the first time systematic inelastic fixed window pressure studies from the neutron backscattering instrument IN16B at the Institut Laue-Langevin (ILL) and use those to test density scaling. Most of the data presented in this paper have been measured in a newly developed pressure cell for performing simultaneous dielectric

and neutron spectroscopy as a function of temperature and pressure,²⁶ thereby expanding the accessible neutron scattering to include longer time scales while assuring that the data are collected under exactly the same experimental conditions.

In this paper, we present scaling of the α -relaxation on pico- to millisecond time scales for three different systems, two simple van der Waals liquids and a more complex hydrogen-bonding liquid, studied with neutron and dielectric spectroscopy. We begin by introducing experimental details in Sec. II. Data are presented in Sec. III containing three subsections, one for each sample, followed by the discussion in Sec. IV.

II. EXPERIMENTAL DETAILS

The three samples presented in this paper are two van der Waals liquids, isopropyl benzene (cumene) and 5-polyphenyl ether (PPE) and the hydrogen-bonding liquid dipropylene glycol (DPG) (Fig. 1). Cumene and DPG were purchased from Sigma Aldrich and PPE from Santolubes, and all three samples were used as acquired. The two van der Waals liquids are considered simple in the sense that they do not possess pronounced secondary relaxations or intra-molecular motion visible on either subnanosecond time scales in the neutron signal or in the dielectric signal²⁷ and have previously been shown to have behavior in agreement with predictions from isomorph theory.^{19,25,28} The hydrogen-bonding liquid DPG represents a complex system with directional bonding, a clear excess wing visible in the dielectric signal²⁹ and methyl-group rotation observable on nanosecond time scales with neutron spectroscopy. Furthermore, the dynamics of DPG respond fairly well on applied pressure in comparison to most hydrogen-bonding liquids, which in general show only little pressure dependence. The molecules are sketched in Fig. 1, and details about the samples can be found in Table I.

The data presented in this paper have been measured at the Institut Laue-Langevin (ILL) using the neutron backscattering

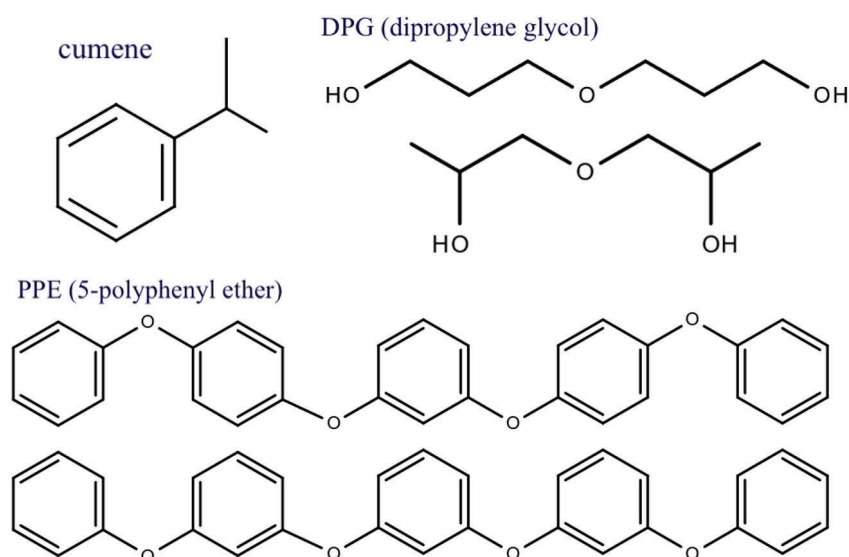


FIG. 1. Sketches of the molecular structure of the three samples studied in this paper. DPG and PPE are mixtures of isomers.

TABLE I. Details on the three samples: cumene (isopropyl benzene), PPE (5-polyphenyl ether), and DPG (dipropylene glycol). The fragility, m , is a measure of the super-Arrhenius behavior introduced by Angell:³⁴ $m = \left. \frac{d \log_{10} \tau(T)}{d(T_g/T)} \right|_{T_g}$.

	$T_g(P_{\text{amb}})$ [K]	m	γ	dT_g/dP [K/MPa]	References
Cumene	126	70	4.8	0.085	25 and 30
PPE	245	80	5.5	0.18	25, 31, and 32
DPG	195	65	1.5	0.075	21, 25, and 33

instruments IN16B and IN13 and the neutron time-of-flight instrument IN5.^{35,36} The time scale of the neutron experiments is determined by the energy resolution and the energy transfer of the neutron instruments; the coarser the energy resolution, the faster the time scale. We measured cumene and DPG on IN16B, accessing nanosecond dynamics with the standard Si(111) setting with $\lambda = 6.271 \text{ \AA}$ in the Q -range from 0.4 to 1.8 \AA^{-1} with an energy resolution of $\sim 0.75 \text{ \mu eV}$ corresponding to nanosecond time scales in the energy range $\pm 30 \text{ \mu eV}$. The elastic intensity of cumene was also measured using the backscattering instrument IN13 with an energy resolution of 8 \mu eV in the Q -range $0.2\text{--}4.9 \text{ \AA}^{-1}$, i.e., one order of magnitude faster than IN16B. Cumene and PPE were both measured on IN5 with a wavelength of 5 \AA and with an energy resolution of 0.1 meV corresponding to a time scale of $\sim 10 \text{ ps}$, i.e., two orders of magnitude faster than IN16B, in the Q -range from 1.2 to 1.9 \AA^{-1} binned in steps of 0.1 \AA^{-1} in the energy range $\pm 2 \text{ meV}$. Full spectra of cumene were also measured using IN5 with wavelength 8 \AA and with energy resolution 0.015 meV accessing a time scale of roughly 0.1 ns in the Q -range from 0.5 to 1.2 \AA^{-1} in the energy range $\pm 1 \text{ meV}$. All data reduction, subtraction of background, normalisation to monitor and vanadium, corrections for cell geometry, and instrument efficiency have been done in the neutron data treatment and evaluation program LAMP.³⁷ Except for the IN16B data on cumene, all data were measured in a newly developed pressure cell for doing simultaneous dielectric and neutron spectroscopy under high pressure.²⁶ The temperature range for the high-pressure cell is $2\text{--}320 \text{ K}$ and is controlled by the standard orange cryostat available at the ILL. The pressure range is $0.1\text{--}500 \text{ MPa}$. Both the temperature and pressure ranges are determined by the aluminum alloy of the high-pressure cell, which is used because of its low background in the neutron signal. This new sample cell is a unique tool for combining techniques, thereby accessing dynamics on different time scales with high precision, making sure that data are collected under exactly the same sample conditions.

We utilise fast switching between the elastic and inelastic fixed window scans unique for the backscattering instrument IN16B (Ref. 38). These scans offer a fast overview of how a parameter such as temperature or pressure in the full Q -range affects the dynamics. The inelastic fixed energy window scan (IFWS) data presented in this paper were measured with an energy offset at 2 \mu eV and a maximum is observed when the spectral weight at the offset energy is the highest as a relaxational process passes through the instrument window, for example, caused by an increase of the quasielastic broadening. The nature of the dynamics, whether it is a local

process or of translational character, can be determined from the Q -dependence. That is, if a relaxation shows change in the Q -dependence as a function of temperature or pressure, it is a delocalised translational motion, whereas a local process will be independent of Q as a function of pressure or temperature.³⁹ All spectra are shown summed over Q for better statistics since we generally observe the same trend for all values of Q , unless otherwise stated. More data and details on samples and data are available in Ref. 40.

Equations of state to calculate the density at various state points for cumene are from Ref. 30, for PPE from Ref. 32, and for DPG from Ref. 41. The scaling exponents used for testing density scaling for the three samples were found in previous publications: Ransom and Oliver³⁰ measured the glass transition temperature of cumene in a large pressure range, up to $\sim 4 \text{ GPa}$, and found $\gamma = 4.8$ and used this to density scale light scattering data⁴² and viscosity data.^{43,44} The scaling exponent for PPE was found from dielectric data to be $\gamma = 5.5$ (Ref. 32) and used in scaling of dielectric spectra.²⁸ The two van der Waals liquids complement each other in terms of experimental accessibility: cumene has a low glass transition temperature which means that the α -relaxation reaches subnanoseconds, probed by our scattering experiments, within the (T, P) -range accessible by our sample cell, and furthermore, cumene crystallizes easily in the range between the melting point and the glass transition. PPE, on the other hand, does not crystallize and we can therefore easily study dynamics in the viscous dynamic range, whereas the α -relaxation is too slow within the (T, P) -limits of our equipment compared to the neutron time scales. The hydrogen-bonding liquid DPG was found to have a scaling exponent of $\gamma = 1.5$ (Ref. 33), a quite low value of γ compared to the two van der Waals liquids, but typical for hydrogen-bonding liquids.^{6,11,45} This scaling exponent allows for scaling of the α -relaxation in the range from microseconds to milliseconds,²¹ while it does not provide a satisfactory collapse for dynamics close to the glass transition.

As mentioned earlier, according to isomorph theory, the relevant quantities to investigate are in reduced units, which are per definition dimensionless (presented with a tilde). Examples of length and time units, l_0 and t_0 , respectively, used in this paper are

$$\begin{aligned} l_0 &= \rho^{-1/3}, \\ t_0 &= \rho^{-1/3} (m_p/k_B T)^{1/2}, \end{aligned} \quad (1)$$

where m_p is the average particle mass and ρ is the number density. For length, wave vector, and frequency, respectively, the reduced dimensionless units denoted with a tilde are then given by

$$\begin{aligned} \tilde{\mathbf{r}} &= \mathbf{r}/l_0 = \mathbf{r}\rho^{1/3}, \\ \tilde{Q} &= Q l_0 = Q\rho^{-1/3}, \\ \tilde{\omega} &= \omega t_0 = \omega \rho^{-1/3} (m_p/k_B T)^{1/2}. \end{aligned} \quad (2)$$

The frequency unit ω multiplied by \hbar corresponds to the energy transfer. We assume that the average particle mass is constant and set $m_p = k_B = 1$. Effectively, the reduced unit for energy transfer thus becomes

$$\tilde{\omega} = \omega \rho^{-1/3} T^{-1/2}, \quad (3)$$

where ρ is now the volumetric mass density. In the dynamic range investigated in this paper, the change in density is in the percent range; thus, the inverse of the cubic root of the density will only have a small effect on the scaling of the energy transfer. Plotting data in reduced energy units will therefore mainly be affected by temperature changes. The scaling has a visible effect only for higher energy transfer, and we will therefore ignore the reduced units for the low frequency IFWS in Sec. III. Expressing Q in reduced units will result in changes of around 1%, which will be within the uncertainty of the data and is therefore also neglected.

III. RESULTS

In this section, we present high-pressure neutron scattering data from the two van der Waals liquids, cumene and PPE,

and the hydrogen-bonding liquid, DPG, presented in three subsections according to the sample.

A. van der Waals liquid—cumene

First, we present the fixed window scans from IN16B on cumene in Fig. 2, i.e., on nanosecond time scales. In the top panel, the elastic and inelastic fixed energy window scan (EFWS and IFWS) intensities are shown as a function of pressure for the three isotherms. From the EFWS ($\Delta E = 0 \mu\text{eV}$), the intensity is observed to increase on compression as the mobility decreases moving towards the glass transition. In the IFWS ($\Delta E = 2 \mu\text{eV}$), a maximum is observed in the intensity as a function of pressure as the α -relaxation moves through the instrument window upon compression.

Density scaling predicts that the control parameter of the dynamics is $\Gamma = \rho^\gamma/T$ and we therefore plot the three isotherms

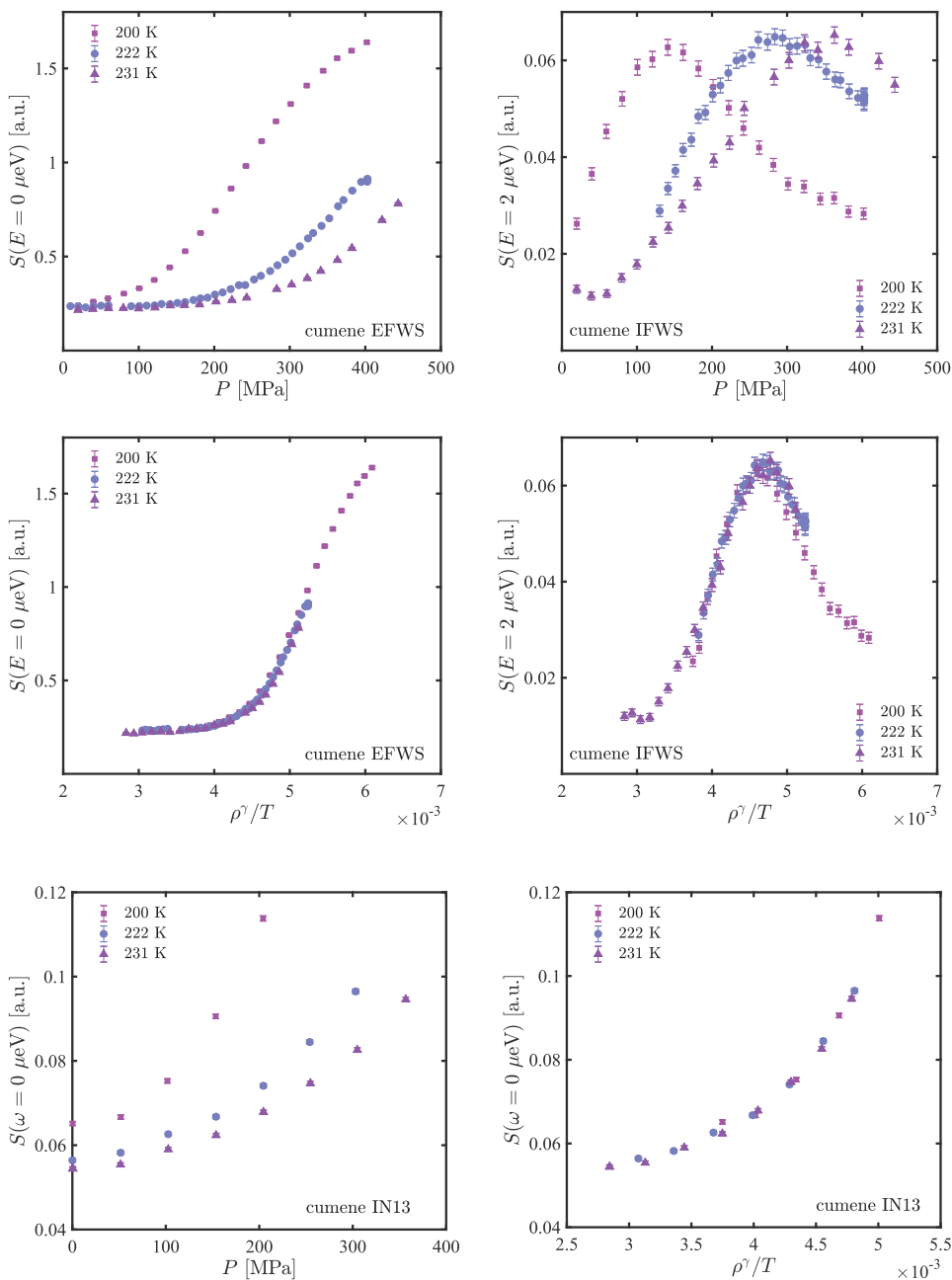


FIG. 2. EFWS (left) and IFWS (right) from IN16B (~ 1 ns) on cumene summed over Q . Intensity of EFWS and IFWS plotted for three isotherms (200 K, 222 K, and 231 K) as a function of pressure (top) and as a function of $\Gamma = \rho^\gamma/T$ with $\gamma = 4.8$ (bottom).

FIG. 3. Elastic intensity of cumene from IN13 (~ 0.1 ns) summed over Q . Left: three isotherms (200 K, 222 K, and 231 K) as a function of pressure. Right: Density scaling of left plotted as a function of $\Gamma = \rho^\gamma/T$, $\gamma = 4.8$.

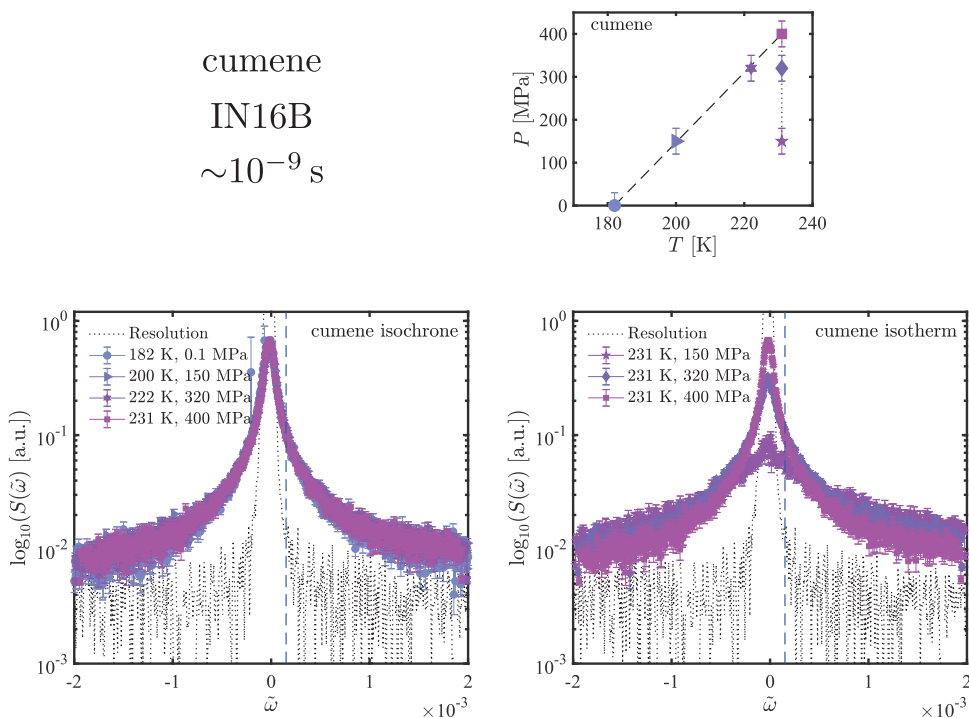


FIG. 4. Spectra of cumene from IN16B (\sim ns) summed over Q . The (T, P) -phase diagram shows the studied state points for the isochrone as determined from the fixed window scan on IN16B and an isotherm at 231 K. The blue dashed line in the spectra corresponds to an energy offset of $2 \mu\text{eV}$ used for the inelastic fixed window scans.

from the FWS on IN16B as a function of ρ^γ/T in the bottom panel of Fig. 2 using the scaling exponent $\gamma = 4.8$ determined by Ransom and Oliver.³⁰ We observe how the data collapse to just one curve for both the EFWS and the IFWS. The same is observed for the elastic intensity from IN13 (Fig. 3), also a backscattering instrument, with an energy resolution that corresponds to a time scale one order of magnitude faster than that of IN16B. We are able to express the nanosecond dynamics along three isotherms in the equilibrium liquid with the α -relaxation on nanosecond time scales as a function of the control parameter $\Gamma = \rho^\gamma/T$ using a γ value found in the supercooled liquid at the glass transition. According to isomorph theory, the scaling exponent, γ , is allowed to change with temperature and density and to depend on the dynamic range and it has, of course, itself an uncertainty. With this type of experiment and uncertainty, we are not able to determine whether γ is state-point dependent. In fact, the data can be made to collapse using values of γ in the range from 4.2 to 4.8. This type of analysis does not offer a precise way of determining γ . However, within the experimental uncertainty that

we have for this kind of experiment, e.g., knowing the exact temperature, we note how well the value found by Ransom and Oliver³⁰ in the highly viscous liquid using completely different experimental techniques works here in the equilibrium liquid and therefore use $\gamma = 4.8$ throughout this paper for cumene.

For the interpretation of the fixed window scans, we assume that by knowing the intensity of the elastic peak ($\Delta E = 0 \mu\text{eV}$) and the intensity at some offset energy, in this case, $\Delta E = 2 \mu\text{eV}$, we have enough information to interpret how the overall spectral shape and linewidth or quasielastic broadening changes with some variable, in this case T and P . Therefore, an indirect assumption of isochronal superposition goes into this interpretation; i.e., we assume that the linewidth of the spectral shape changes in a similar way for temperature and pressure. This assumption can be tested by determining an isochrone from the EFWS and IFWS along three isotherms from IN16B (Fig. 2, top) by identifying the same level of intensity on the curves for the three isotherms and investigating the full spectra. In Fig. 4, we present the full spectra from IN16B measured

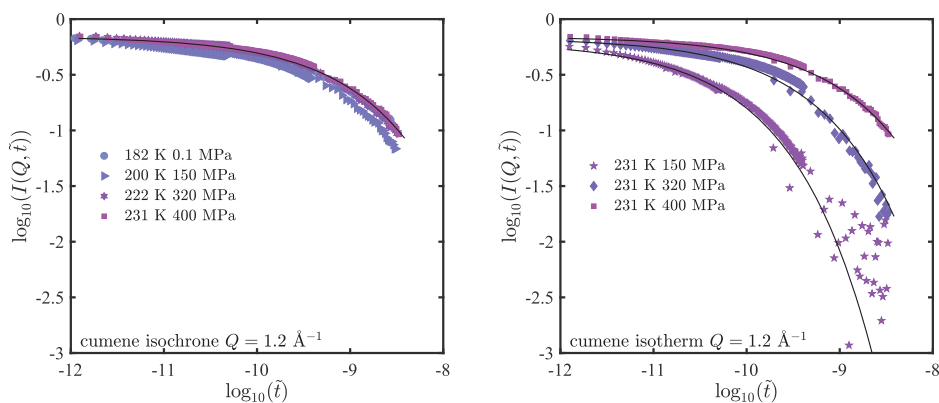


FIG. 5. Fourier transform of combined cumene spectra from IN16B and IN5 with $\lambda = 5 \text{ \AA}$ and 8 \AA for $Q = 1.2 \text{ \AA}^{-1}$. The full line is a stretched exponential fit to data from IN16B and IN5 with $\lambda = 8 \text{ \AA}$ and 5 \AA and $\sim 0.1 \text{ ns}$ and $\sim 10 \text{ ps}$, respectively.

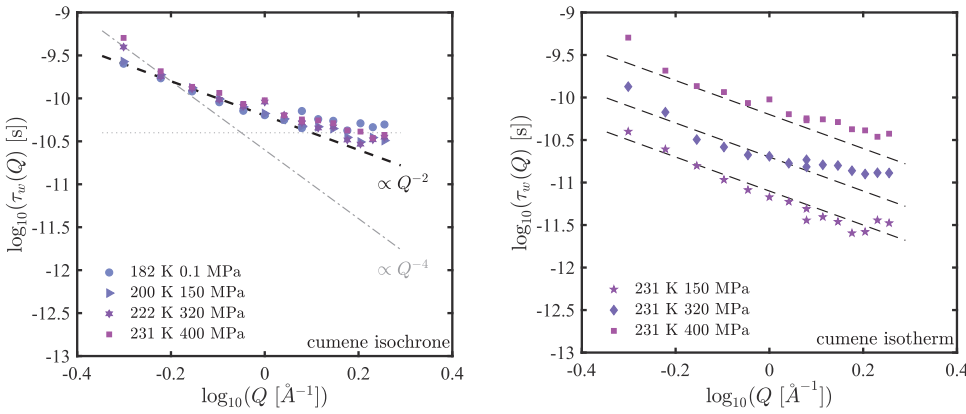


FIG. 6. The relaxation time τ_w as a function of Q for cumene obtained from a stretched exponential fit to the Fourier transformed combined spectra from IN5 and IN16B along an isochrone and an isotherm. An example of the fit is shown as black lines in Fig. 5. The dashed lines correspond to a Q^{-2} dependence of the relaxation time.

along the isochrone determined from the FWS and an isotherm for comparison. The studied state points are shown in the (T, P) -phase diagram. We observe an invariance of the spectral shape and quasielastic broadening along the isochrone. For the isotherm, we observe less elastic intensity and more relaxation in the instrument window with decreasing pressure as the α -relaxation time becomes faster. The former means that just one spectrum at a given (T, P) gives the spectral shape and the FWS, which give the temperature and pressure dependence of the width, and we are able to predict the spectral shape and linewidth along all state points that are isochronal to that spectrum.

At the same state points as presented in Fig. 4 for IN16B, spectra were measured on IN5 at two different resolutions, where we observed the same trend. In Fig. 5, we show the Fourier transformed combined spectra of cumene from IN16B and IN5 with $\lambda = 8$ and 5 \AA at $Q = 1.2 \text{ \AA}^{-1}$ and $\sim 0.1 \text{ ns}$ and $\sim 10 \text{ ps}$, respectively. The Fourier transformed data have been corrected for resolution by merely dividing by the low-temperature spectrum of cumene for each spectrometer and wavelength. The total dynamic range spans close to four decades, and we observe a good degree of invariance for the intermediate scattering function, $I(Q, t)$, along the isochrone determined from the FWS on IN16B that is shown on the same scale as the isotherm for comparison. For the isotherm, we observe as expected the relaxation time decreasing as pressure is released.

Relaxation processes in disordered systems are typically fitted with a stretched exponential as a phenomenological

fitting function. We fitted the intermediate scattering functions with a stretched exponential as a function of Q ,

$$I(Q, t) = A e^{-\left(\frac{t}{\tau_w(Q)}\right)^\beta}, \quad (4)$$

where A is the amplitude, τ_w is the Q -dependent relaxation time, and β is the stretching parameter. The stretching parameter was fixed at $\beta = 0.5$ for all spectra as this gave the best fits, which indicates that the shape of all the spectra, independent of temperature and pressure, is the same, which means that isochronal superposition of the α -relaxation becomes an evident observation.

The Q -dependence of the relaxation time is shown in Fig. 6 for the isochrone determined from the FWS on IN16B, and for comparison, the Q -dependence of an isotherm is also shown. The relaxation time is observed to be fairly invariant along the isochrone, while the relaxation time is observed to slow down with increased pressure along the isotherm. For both the isochrone and the isotherm, the relaxation time is observed to become faster with increasing Q , showing a Q^{-2} -dependence in a large part of the accessible Q -range. This behavior suggests a Gaussian behavior which is observed to deviate for high Q , i.e., short distances, where the relaxation time is observed to flatten out away from the Gaussian behavior resembling, for example, jump-diffusion like motion. At low Q , there might be a slight tendency for the relaxation time to bend off into a $Q^{-2/\beta}$ behavior as suggested in Ref. 46, although this is not clear from these data sets. The Q -dependence observed for cumene suggests translational motion typical for structural relaxation.

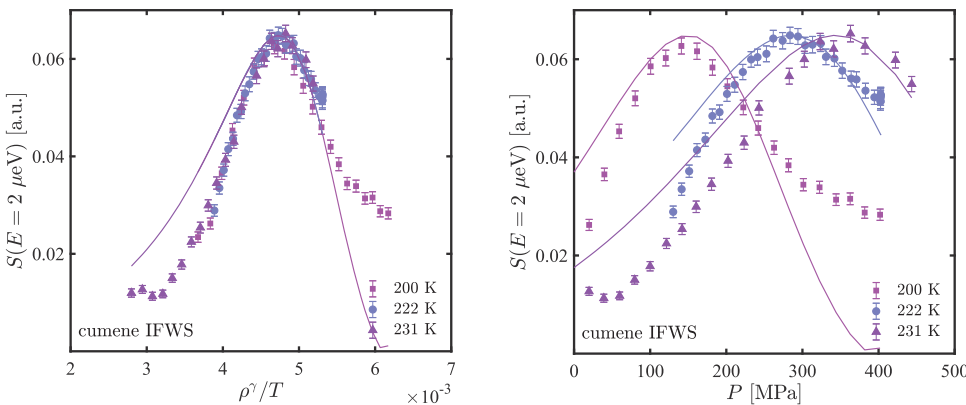


FIG. 7. Comparison of the simple model in Eq. (6) based on the relaxation times obtained from the full cumene spectra and data on three isotherms from IFWS on IN16B (\sim ns). The density scaled IFWS data are shown on the left and as a function of pressure on the right.

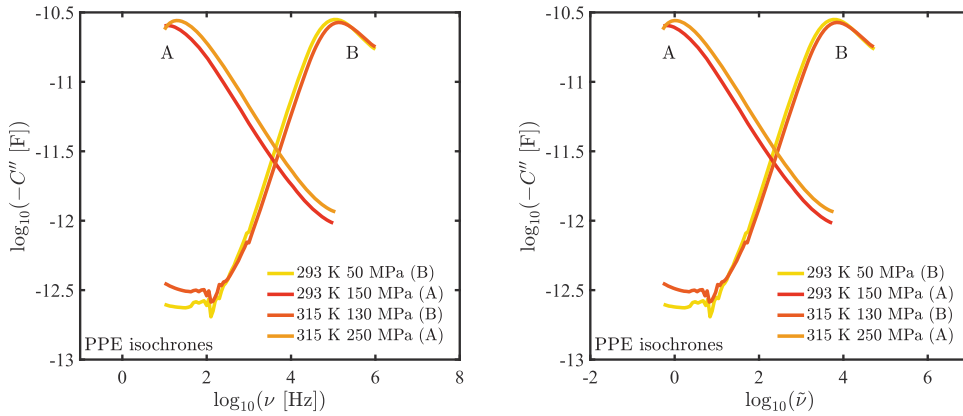


FIG. 8. Two pairs of isochronal state points determined from the dielectric loss peak on PPE measured on IN5, $\lambda = 5 \text{ \AA}$. Relaxation time for isochrone (A) is $\tau_\alpha \approx 10^{-2} \text{ s}$ and for (B) $\tau_\alpha \approx 10^{-6} \text{ s}$. Dielectric loss plotted as a function of frequency on an absolute scale (left) and as a function of the reduced frequency unit (right).

Using the mode-coupling parameters reported in Ref. 42, and an expression for the temperature dependence of the relaxation time reported in Ref. 47, and then substituting $\Gamma = \rho^\gamma/T$ for the temperature dependence and $\Gamma_c = \rho_c^\gamma/T_c$ for the critical temperature, we end up with an expression for the relaxation time

$$\tau = \frac{\tau_0}{((\Gamma - \Gamma_c)/\Gamma_c)^n}, \quad (5)$$

where n is the MCT critical exponent. Note that only the prefactor τ_0 is fitted to the data, and the rest of the parameters are found in Ref. 42. The data are fitted in the equilibrium liquid above the critical temperature, which is reported to be $\sim 160 \text{ K}$ at ambient pressure. We use this expression of the α -relaxation time and then suggest a simple model for our neutron data with a single relaxation process moving through the instrument window at a fixed energy, 2 \mu eV , similar to the IFWS from IN16B. If the relaxation process was an exponential process, this would correspond to a Lorentzian, and we therefore add a phenomenological stretching to account for

the stretched exponential behavior. The simple model is then given by

$$I \propto \frac{\tau^\beta}{1 + (\omega^2 \tau^2)^\beta}. \quad (6)$$

In Fig. 7, we have used this model with the expression for the relaxation time as a function of ρ^γ/T given in Eq. (5) to recreate the IFWS shown as a function of ρ^γ/T and finally as a function of pressure. This model suggests only one distribution of relaxation times and is in qualitative agreement with our data, recreating the position of the maximum of the IFWS from the relaxation time obtained from fits to the full spectra and Eq. (5), thereby supporting our interpretation of the FWS.

B. van der Waals liquid—PPE

The second van der Waals liquid is PPE, which only barely shows relaxation in the IN16B instrument window in the temperature and pressure range accessible with this setup. Instead, PPE data are reported from IN5 at 5 \AA ($\sim 10 \text{ ps}$) in

PPE
IN5, $\lambda = 5 \text{ \AA}$
 $\sim 10^{-11} \text{ s}$

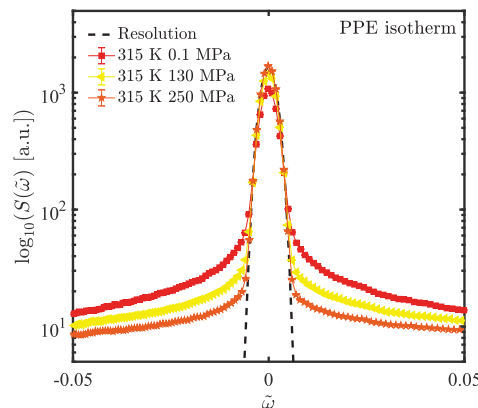
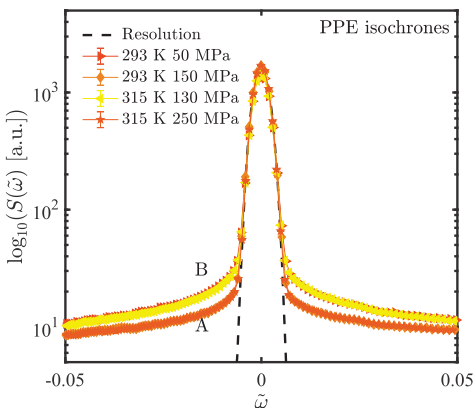
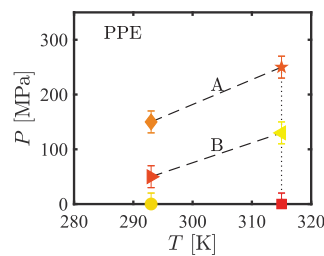


FIG. 9. Spectra of PPE from IN5 at $\lambda = 5 \text{ \AA}$ summed over Q . Top: The phase diagram shows the studied state points as a function of temperature and pressure and indicates the two pair of isochronal state points (A+B). Bottom: Two pairs of isochronal state points found from dielectrics (left) and an isotherm at 315 K for comparison (right).

the combined dielectric and neutron sample cell, i.e., accessing dynamics with neutrons on picosecond time scales. Two pairs of isochronal state points were found with high precision from the dielectric loss peak in the simultaneous dielectric and neutron measurements. The two pairs of isochronal state points are shown in Fig. 8 with α -relaxation times of roughly 10^{-2} s and 10^{-6} s for isochrones (A) and (B), respectively. The dielectric spectra are shown both as a function of frequency on an absolute frequency scale and in reduced frequency units. We observe that within the experimental uncertainty, there is no influence on the relative position of the state points, i.e., isochronal state points on an absolute scale are also isochronal in reduced units. This observation supports the idea of identifying possible isomorphs by isochrones, an approach that was also taken to study the ultraviscous liquid in Ref. 25.

The IN5 neutron spectra are shown in Fig. 9 for the two pairs of isochronal state points (A) and (B). The α -relaxation times of PPE covered here on isochrones and isotherms are located between the α -relaxation time found for cumene in Subsection III A and the glass transition, a dynamic range not accessible in cumene because of crystallization, but readily accessible with PPE. For the isotherm, we observe the dynamics slowing down as the liquid is compressed, i.e., less quasielastic broadening. For the isochronal state points, we observe an invariance of the spectral shape and the quasielastic broadening. This collapse is far from trivial; what we see on picosecond time scales is interpreted as the tail of the α -relaxation stretching over many orders of magnitude, where vibrations and fast relaxation are here merged with the α -relaxation,²⁷ suggesting that the whole relaxation curve is invariant for isochronal state points also in the liquid state.²⁵

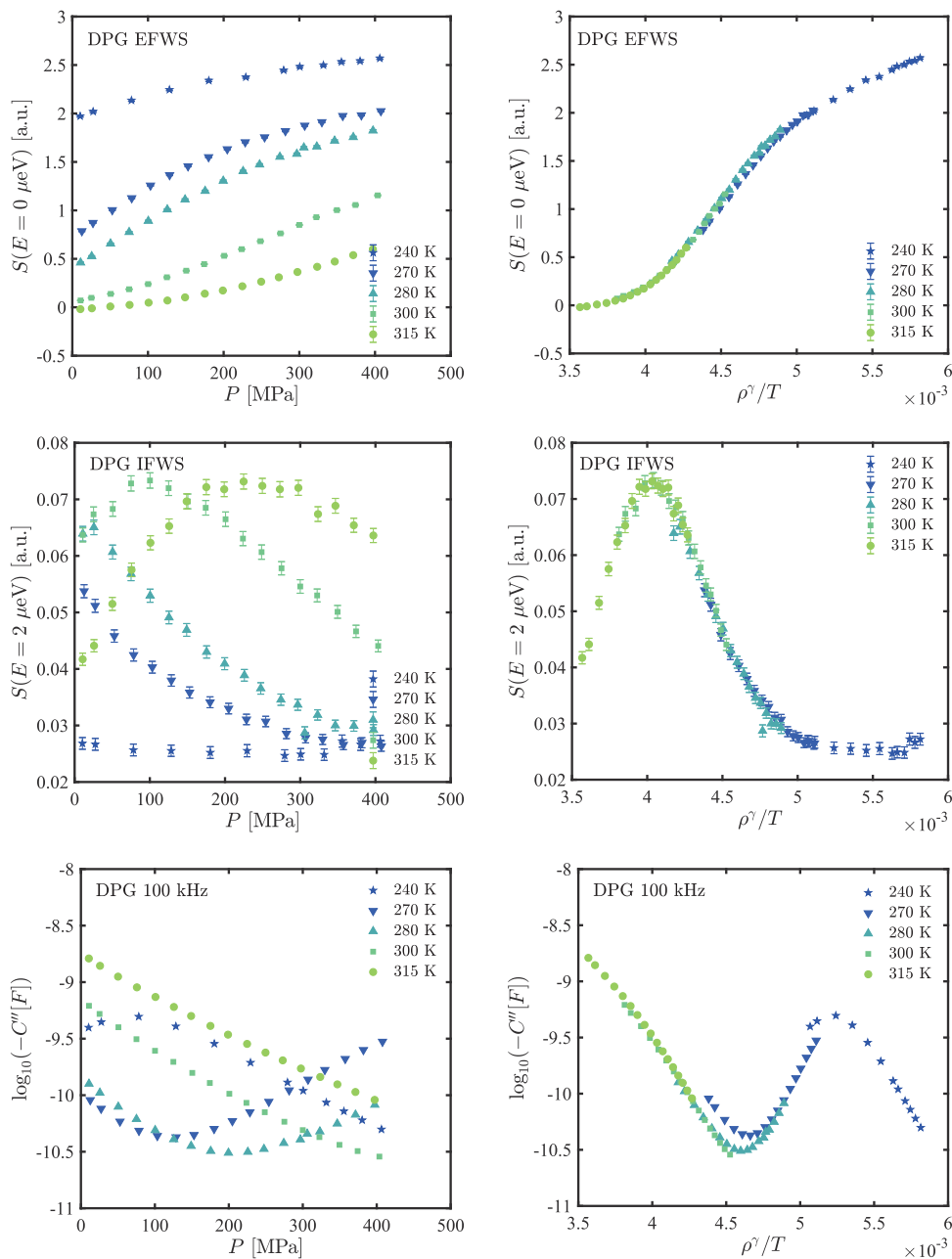


FIG. 10. FWS from IN16B (\sim ns) on DPG summed over Q . Intensity of the EFWS (top) and IFWS (middle) and fixed frequency dielectric loss (bottom) plotted for five isotherms (240 K, 270 K, 280 K, 300 K, and 315 K) as a function of pressure (left) and as a function of $\Gamma = \rho^\gamma/T$ (right).

C. Hydrogen-bonding liquid—DPG

The third set of data that we present is measured on the hydrogen-bonding liquid DPG using IN16B (\sim ns). We present fixed window scans, full spectra, and simultaneously acquired dielectric data, securing the precision of the measurements. In Fig. 10, we show the measured EFWS and IFWS intensity at $\Delta E = 0 \mu\text{eV}$ and $\Delta E = 2 \mu\text{eV}$, respectively, as a function of pressure and as a function of ρ^γ/T using $\gamma = 1.5$ (Ref. 33) for five isotherms and a similar plot with the dielectric loss signal at a fixed frequency of 10^5 Hz. We observe an increase in the EFWS intensity upon compression as the mobility is decreased. From the IFWS, we observe that the high-temperature isotherms go through a maximum, similar to what was observed for cumene (Fig. 2), i.e., the α -relaxation passes through the neutron instrument window. Equivalently, for the low temperature isotherms, the α -relaxation is observed to pass through the fixed frequency of the dielectrics. As the α -relaxation moves out of the dielectric window, we observe DC-conductivity, also evident from the full frequency range in Fig. 11. We observe how the respective intensities can be made to collapse to a master curve for the dynamics on neutron nanosecond time scales when plotted as a function of ρ^γ/T and to some degree for the dielectric signal measured at roughly microsecond time scales.

Just as for cumene, an isochrone was determined from the EFWS and IFWS intensity. In this case, we also have dielectric data showing DC-conductivity and the wing of the

relaxation observed in the dielectrics. A temperature-pressure phase diagram illustrating the studied state points is shown in Fig. 11 along with the full spectra from IN16B and the dielectric signal at those state points. The dielectric signal where mainly DC-conductivity is observed in addition to the tail of the α -relaxation at high frequencies is observed to be invariant along the isochrone determined by neutron fixed window scans at nanosecond time scales. The DC-conductivity and α -relaxation decouple in DPG;²¹ however, we find that the full dielectric spectrum is invariant along the isochrones found from EFWS and IFWS. A correlation between α -relaxation time and the conductivity was also shown in Ref. 6. Our data show that isoconductivity lines and the α -relaxation isochrone coincide, indicating that different dynamic properties depend on the same scaling parameter Γ , even if the temperature and pressure dependence may differ. The full spectral shape and quasielastic broadening of the IN16B data are also observed to be invariant for the isochrone. An isobar is shown for comparison, where we observe the dynamics speeding up as the temperature is increased, causing more broadening and less elastic intensity.

The spectra from IN16B shown in Fig. 11 are all from state points where the α -relaxation is near the time scale of the backscattering instrument window of IN16B, i.e., nanoseconds. In Fig. 12 (top), we present fixed window scans from two isobars, at ambient pressure and at 300 MPa, carried out from the high temperature region, where the α -relaxation is in the instrument window, all the way into the glassy state.

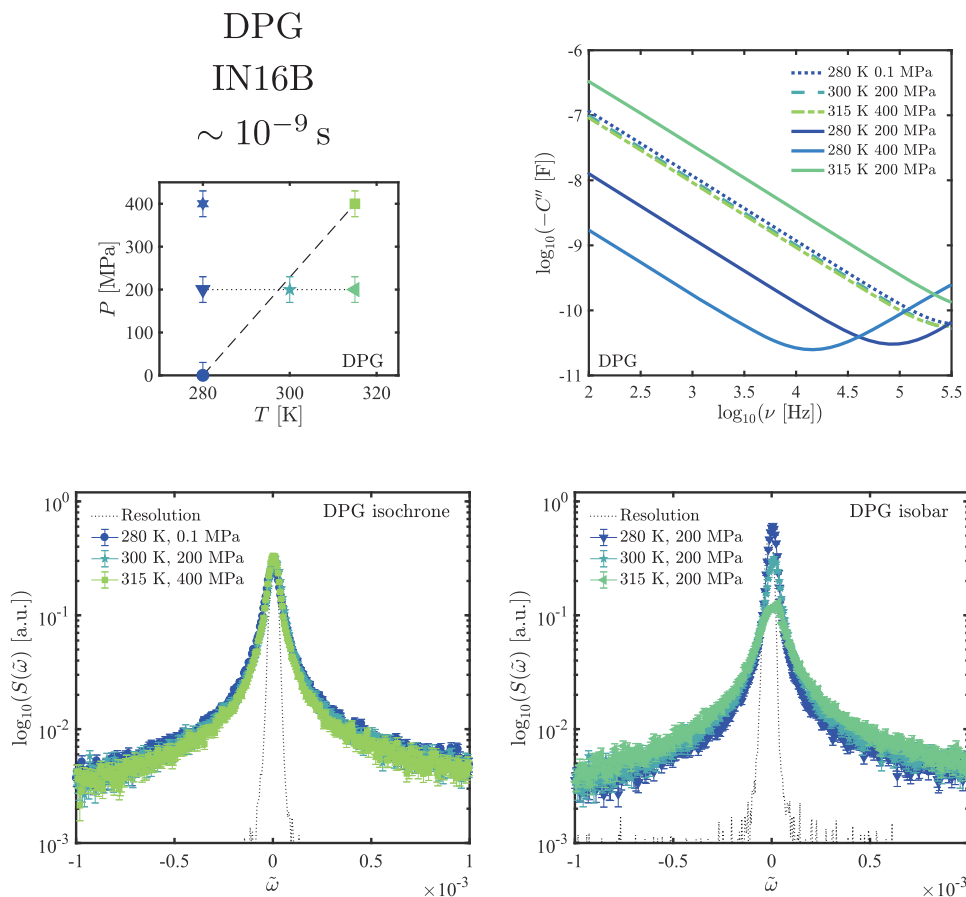


FIG. 11. Top: (T,P) -phase diagram with the studied state points of DPG on IN16B (\sim ns) and the dielectric loss as a function of frequency. Bottom: Spectra of DPG summed over Q showing an isochrone (left) determined from FWS on IN16B and the dielectrics and an isobar for comparison (right).

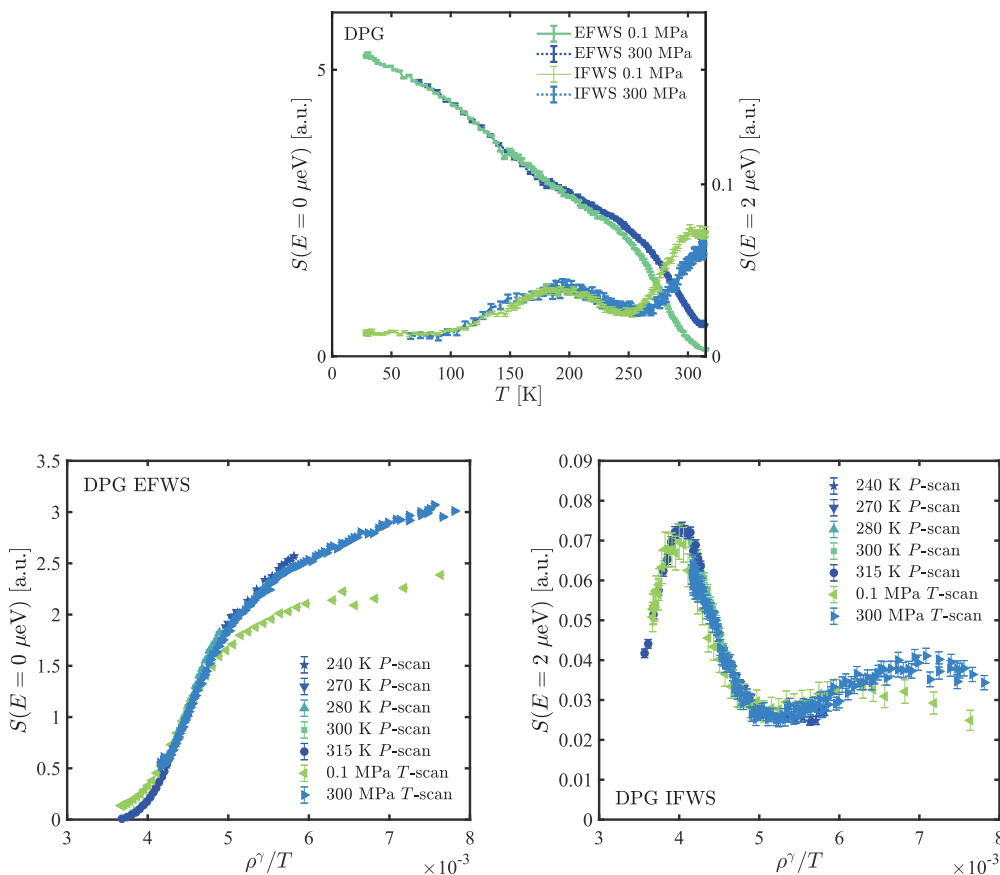


FIG. 12. Top: EFWS and IFWS from IN16B (~ns) on DPG along two isobars at ambient pressure and 300 MPa. Bottom: Density scaling of the EFWS (left) and IFWS (right) that is shown above and in Fig. 10, i.e., for both the isobars and isotherms.

On cooling at IN16B, DPG is observed to have a distinct signal with a maximum close to the glass transition, $T_g(P_{\text{atm}}) = 195$ K. This signal is well separated from the α -relaxation on IN16B which is roughly 100 K higher at ambient pressure. While the α -relaxation with a maximum at ~ 300 K is observed to move upon increased pressure, the second bump at lower temperatures does not respond to pressure, also visible in the weak pressure dependence of the IFWS in the 240 K pressure scan in Fig. 10, which indicates that this contribution is from intra-molecular dynamics.

If we compare the Q -dependence for the isotherm at 240 K to that at 300 K (Fig. 13), we see that for the high temperature isotherm, there is a clear shift of the relaxation

process on compression towards higher Q , indicating that this is of translational character, whereas there is no Q -dependence observed for the isotherm at 240 K, suggesting a local process with a higher intensity at higher Q . This signal most likely stems from the methyl-group rotation of DPG and is manifested in the IFWS as the second broad bump at lower temperatures than the α -relaxation with a maximum around 200 K (Fig. 12). By combining the two isobars with the five isotherms in Fig. 10, we observe that when the EFWS and IFWS are plotted as a function of ρ^γ/T , density scaling breaks down for the methyl-group dynamics and the dynamics can no longer be expressed solely by $\Gamma = \rho^\gamma/T$.

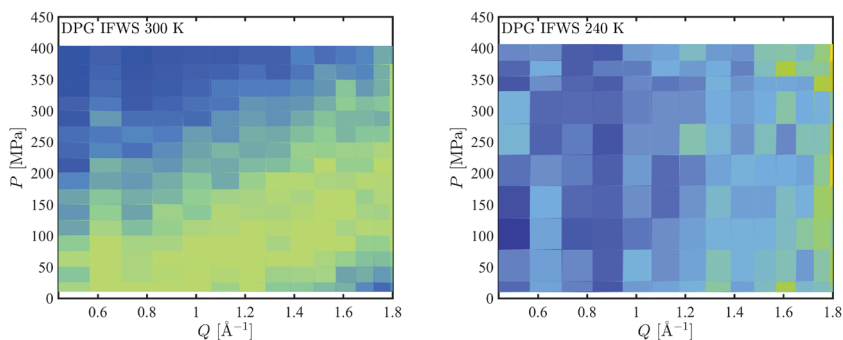


FIG. 13. Q -dependence of the IFWS of two isotherms from IN16B (~ns) on DPG at 300 K (left) and 240 K (right).

IV. DISCUSSION

In Sec. III, we showed how dynamics of the α -relaxation taking place on time scales accessible with neutron and dielectric spectroscopy can be made to collapse into one curve when performing density scaling in the equilibrium liquid. The dynamics covers time scales from picoseconds to milliseconds and suggest that the time scale of the α -relaxation is determined by the control parameter $\Gamma = \rho^\gamma/T$. We have shown isochronal superposition over several decades in time accessed by different spectrometers for the simple van der Waals liquid PPE, i.e., an invariance in the quasielastic broadening on picosecond time scales along isochrones determined from dielectrics. Also, for DPG, we observed that the DC-conductivity visible from dielectrics and the full spectral shape and linewidth were invariant along the isochrone determined from the FWS on IN16B and the dielectric spectra. Cumene was measured and combined at two different neutron spectrometers to cover almost four orders of magnitude in the time domain, which allowed for a more detailed analysis of the relaxation.

The spectral shape of the Fourier-transformed cumene data was fitted with the same stretching exponent $\beta = 0.5$ for all temperatures and pressures, which suggests time-temperature-pressure superposition; i.e., the shape of the α -relaxation is always the same in the equilibrium liquid far from the glass transition. For this liquid, this observation implies an extra level of simplicity that makes the observation of isochronal superposition evident.⁵⁰

Most density scaling studies have been performed in the viscous liquid close to the glass transition. In this study, we move away from the slow-flowing liquid and into the liquid state. The α -relaxation times for cumene and DPG in this study were mainly in the instrument window of IN16B, i.e., on nanosecond time scales. Density scaling for the α -relaxation dynamics was shown for the two liquids with very different values of γ , both reported elsewhere and found in a different dynamic range measured with different techniques. While the scaling exponent γ is allowed to vary, we observe that for cumene, $\gamma = 4.8$ (Ref. 30) works well within the experimental uncertainty that we have to work with. The γ -value of cumene is fairly high, meaning that density plays a much larger role for the dynamics, as compared to the hydrogen-bonding liquid DPG, where the scaling exponent is just $\gamma = 1.5$ (Ref. 33), meaning that the dynamics therefore mainly are affected by temperature.

In agreement with previous observations,^{22–24} we observe density scaling to work well for the tested hydrogen-bonding liquid also when it comes to the α -relaxation. But we observed density scaling to break down for the intra-molecular dynamics of the methyl-group rotation that was identified from the lack of pressure response and the Q -dependent signal. Previously, we have observed isochronal superposition to break down for the hydrogen-bonding liquid DPG along the glass transition when fast relaxation and vibrations were completely separated from the α -relaxation.²⁵

The fact that we observe density scaling to break down in this study for the intra-molecular motion in DPG is in agreement with observations from molecular dynamics

simulations.^{48,49} Spring-like bonds were introduced as intramolecular motion and what was referred to as pseudo-isomorphs were recovered when only the intermolecular dynamics were treated, i.e., the scaling only worked for intermolecular motion. A partly deuterated DPG sample that would mask the methyl-group rotation in the neutron signal would therefore be an obvious next approach to test whether density scaling in this way can be restored for the full dynamic range.

ACKNOWLEDGMENTS

This work was supported by the Danish Council for Independent Research (Sapere Aude: Starting Grant). For technical support, we acknowledge the people in the workshop of IMFUFA and participants involved in the long-term proposal (LTP-6-7) at the ILL; Eddy Lelièvre-Berna, Julien Gonthier, cryogenics and high-pressure from the SANE group, and instrument responsables Judith Peters on IN13 and Jacques Olivier on IN5.

- ¹L. Berthier and G. Biroli, *Rev. Mod. Phys.* **83**, 587 (2011).
- ²M. D. Ediger and P. Harrowell, *J. Chem. Phys.* **137**, 080901 (2012).
- ³A. Arbe, F. Alvarez, and J. Colmenero, *Soft Matter* **8**, 8257 (2012).
- ⁴S. Khodadadi and A. P. Sokolov, *Soft Matter* **11**, 4984 (2015).
- ⁵P. Luo, P. Wen, H. Y. Bai, B. Ruta, and W. H. Wang, *Phys. Rev. Lett.* **118**, 225901 (2017).
- ⁶C. M. Roland, S. Hensel-Bielowka, M. Paluch, and R. Casalini, *Rep. Prog. Phys.* **68**, 1405 (2005).
- ⁷A. Tölle, *Rep. Prog. Phys.* **64**, 1473 (2001).
- ⁸B. Frick, C. Alba-Simionesco, K. Andersen, and L. Willner, *Phys. Rev. E* **67**, 051801 (2003).
- ⁹K. L. Ngai, R. Casalini, S. Capaccioli, M. Paluch, and C. M. Roland, *J. Phys. Chem. B* **109**, 17356 (2005).
- ¹⁰C. Dreyfus, A. Aouadi, J. Gapinski, M. Matos-Lopes, W. Steffen, A. Patkowski, and R. M. Pick, *Phys. Rev. E* **68**, 011204 (2003).
- ¹¹R. Casalini and C. M. Roland, *Phys. Rev. E* **69**, 062501 (2004).
- ¹²C. Alba-Simionesco, A. Cailliaux, A. Alegría, and G. Tarjus, *Europhys. Lett.* **68**, 58 (2004).
- ¹³N. Gnan, T. B. Schröder, U. R. Pedersen, N. P. Bailey, and J. C. Dyre, *J. Chem. Phys.* **131**, 234504 (2009).
- ¹⁴J. C. Dyre, *J. Phys. Chem. B* **118**, 10007 (2014).
- ¹⁵N. P. Bailey, U. R. Pedersen, N. Gnan, T. B. Schröder, and J. C. Dyre, *J. Chem. Phys.* **129**, 184507 (2008).
- ¹⁶U. R. Pedersen, G. H. Peters, T. B. Schröder, and J. C. Dyre, *J. Phys. Chem. B* **114**, 2124 (2010).
- ¹⁷T. S. Ingebrigtsen, T. B. Schröder, and J. C. Dyre, *J. Phys. Chem. B* **116**, 1018 (2012).
- ¹⁸J. C. Dyre, *Rev. Mod. Phys.* **78**, 953 (2006).
- ¹⁹L. Roed, D. Gundermann, J. C. Dyre, and K. Niss, *J. Chem. Phys.* **139**, 101101 (2013).
- ²⁰S. Hensel-Bielowka, S. Pawlus, C. Roland, J. Ziolo, and M. Paluch, *Phys. Rev. E* **69**, 050501 (2004).
- ²¹K. Grzybowska, S. Pawlus, M. Mierzwa, M. Paluch, and K. L. Ngai, *J. Chem. Phys.* **125**, 144507 (2006).
- ²²K. Adrjanowicz, J. Pionteck, and M. Paluch, *RSC Adv.* **6**, 49370 (2016).
- ²³F. Puosi, O. Chulkin, S. Bernini, S. Capaccioli, and D. Leporini, *J. Chem. Phys.* **145**, 234904 (2016).
- ²⁴M. Romanini, M. Barrio, R. Macovez, M. D. Ruiz-Martin, S. Capaccioli, and J. L. Tamarit, *Sci. Rep.* **7**, 1346 (2017).
- ²⁵H. W. Hansen, A. Sanz, K. Adrjanowicz, B. Frick, and K. Niss, *Nat. Commun.* **9**, 518 (2018).
- ²⁶A. Sanz, H. W. Hansen, B. Jakobsen, I. H. Pedersen, S. Capaccioli, K. Adrjanowicz, M. Paluch, J. Gonthier, B. Frick, E. Lelièvre-Berna *et al.*, *Rev. Sci. Instrum.* **89**, 023904 (2018).
- ²⁷H. W. Hansen, B. Frick, T. Hecksher, J. C. Dyre, and K. Niss, *Phys. Rev. B* **95**, 104202 (2017).
- ²⁸W. Xiao, J. Tofteskov, T. V. Christensen, J. C. Dyre, and K. Niss, *J. Non-Cryst. Solids* **407**, 190 (2015).

- ²⁹R. Casalini and C. M. Roland, *Phys. Rev. B* **69**, 094202 (2004).
- ³⁰T. C. Ransom and W. F. Oliver, *Phys. Rev. Lett.* **119**, 025702 (2017).
- ³¹T. Hecksher, N. B. Olsen, K. A. Nelson, and J. C. Dyre, *J. Phys. Chem.* **138**, 12A543 (2013).
- ³²D. Gundermann, “Testing predictions of the isomorph theory by experiment,” Ph.D. thesis, Roskilde University, DNRF Centre “Glass & Time,” 2013.
- ³³A. Grzybowski, K. Grzybowska, J. Ziolo, and M. Paluch, *Phys. Rev. E* **74**, 041503 (2006).
- ³⁴C. Angell, *J. Non-Cryst. Solids* **131**, 13 (1991).
- ³⁵Exp.6-05-961, <https://doi.ill.fr/10.5291/ILL-DATA.6-05-961>.
- ³⁶LTP-6-7, <https://doi.ill.fr/10.5291/ILL-DATA.LTP-6-7>.
- ³⁷I. Laue-Langevin, LAMP, the large array manipulation program, http://www.ill.eu/data_treat/lamp/the-lamp-book.
- ³⁸B. Frick, J. Combet, and L. van Eijck, *Nucl. Instrum. Methods Phys. Res., Sect. A* **669**, 7 (2012).
- ³⁹M. Bée, *Quasielastic Neutron Scattering—Principles and Applications in Solid State Chemistry, Biology and Materials Science* (Adam Hilger, 1988).
- ⁴⁰H. W. Hansen, “Dynamics of glass-forming liquids: Will theory and experiment ever meet?,” Ph.D. thesis, Roskilde University, 2018.
- ⁴¹A. Grzybowski, K. Grzybowska, M. Paluch, A. Swietly, and K. Koperwas, *Phys. Rev. E* **83**, 041505 (2011).
- ⁴²G. Li, J. H. E. King, W. F. Oliver, C. A. Herbst, and H. Z. Cummins, *Phys. Rev. Lett.* **74**, 2280 (1995).
- ⁴³A. J. Barlow, J. Lamb, and A. J. Matheson, *Nucl. Instrum. Methods Phys. Res., Sect. A* **292**, 322 (1966).
- ⁴⁴A. C. Ling and J. E. Willard, *J. Phys. Chem.* **72**, 1918 (1968).
- ⁴⁵K. Niss and C. Alba-Simionesco, *Phys. Rev. B* **74**, 024205 (2006).
- ⁴⁶J. Colmenero, A. Arbe, and A. Alegria, *Phys. Rev. Lett.* **71**, 2603 (1993).
- ⁴⁷W. Götzke and L. Sjögren, *J. Phys. C: Solid State Phys.* **20**, 879 (1987).
- ⁴⁸A. A. Veldhorst, J. C. Dyre, and T. B. Schröder, *J. Chem. Phys.* **143**, 194503 (2015).
- ⁴⁹A. E. Olsen, J. C. Dyre, and T. B. Schröder, *J. Chem. Phys.* **145**, 241103 (2016).
- ⁵⁰K. Niss and T. Hecksher, “Perspective: Searching for simplicity rather than universality in glass-forming liquids,” *J. Chem. Phys.* (to be published).